Supplementary Materials

Materials and methods

TPP-1 was purchased from Peptide International (Louisville, USA). All chemicals were from Wako Pure Chemical Industries (Osaka, Japan) or Sigma-Aldrich (St. Louis, MI, USA). ^{64}Cu and ^{18}F were produced at the National Institute of Radiological Science (Chiba, Japan) with 98% radionuclidic purity. All radio-HPLC analysis for the tracers was performed using a JASCO HPLC system (JASCO, Tokyo, Japan) coupled with a YMC-Triat-C18 column (4.6 mm i.d. × 150 mm, 5 μm, Waters, Milford, MA, USA). A flow rate of 1 mL/min was used. The gradient started with 90% solvent A (0.1% trifluoroacetic acid [TFA] in water) and 10% solvent B (0.1% TFA in acetonitrile [MeCN]), and 20 min later, ended with 0% solvent A and 100% solvent B. Effluent radioactivity was measured using a NaI (Tl) scintillation detector system (Ohyo Koken Kogyo, Tokyo, Japan). A 1480 Wizard autogamma counter (PerkinElmer, Waltham, MA, USA) was used to measure radioactivity, as expressed in counts of radioactivity per minute (CPM), accumulating in cells and animal tissues. A dose calibrator (IGC-7 Curiemeter; Aloka, Tokyo, Japan) was used for the other radioactivity measurements.

Preparation of radiolabeled tracers

For ^{18}F labeling

Ninety-five percent-enriched ^{18}O-H_2O was used for irradiation for the production of ^{18}F by the $^{18}O(p, n)^{18}F$ nuclear reaction using a CYPRIS HM-18 cyclotron (Sumitomo Heavy Industries, Tokyo, Japan). ^{18}F-Fluoride was purified by elution from a Sep-Pak Light QMA cartridge (Waters) with 0.5 mL of 0.4 M $KHCO_3$, and a 200 μL fraction with an activity of ^{18}F (740-1100 MBq) was collected. The pH value of the ^{18}F solution was adjusted to 4 with 12 μL of metal-free glacial acetic acid. Ten microliters of 6 mM $AlCl_3$ in sodium acetate buffer (0.1 M, pH 4.1) was then added and heated at 100°C for 15 min to form the Al^{18}F complex. After cooling to RT, 100 μL of 0.67 mM TPP-1-NOTA dissolved in sodium acetate buffer was added and further heated at 80°C for 15 min for chelating of Al^{18}F by NOTA. The reaction mixture was diluted with 200 μL of water-acetonitrile (9: 1, v/v) containing 0.1% TFA and was purified with RP-HPLC (solvent A=0.1% TFA in water, solvent B=0.1% TFA in acetonitrile, flow rate=1.5 mL/min, linear gradient=10 to 100% solvent B in 20 min. The fraction containing the ^{18}F-labeled peptide was collected and dried by a nitrogen bubbling device. The synthesis of [^{18}F]AlF-PEG-TPP-1 was referred to the previous paper.[1]

For ^{64}Cu labeling

TPP-1-NOTA peptide was radiolabeled with $^{64}CuCl_2$. (National Institute of Radiological Sciences, Japan) 20 μg of TPP-1-NOTA in 20 μl of 0.1 M sodium acetate buffer (pH=4.1) was reacted with ~370 MBq (10 mCi) of the neutralized $^{64}CuCl_2$ solution at 80°C for 10 min. After incubation, the reaction mixture was purified with RP-HPLC. The synthesis of [^{64}Cu]-PEG-TPP-1 was referenced the previous paper.[1]

***In vitro* Stability assays**

The stability of tracers in saline and in mouse serum was used the same protocol as before.[2] Ten microliters (~100 μCi) of tracers was added to 90 μl of mouse serum (freshly prepared) and incubated at 37°C with slight agitation for a designated time. Aliquots were removed at each time point and 100 μl of acetonitrile and water (1:1, v/v) was added and centrifuged for 10 min with 10,000 rpm. The supernatant was analyzed using HPLC. For HPLC, the analysis used an additional guard column, (Phenomenex Security Guard 3.00 mm I.D.) for the protection of the C-18 column. For stability in saline, the tracers were

incubated in saline (>90%, v), then aliquots were removed at each time point for HPLC analysis.

***In vitro* stability assay**

For in vivo stability examination, tracers after formulation (in saline) was injected into normal mice through the tail vein (intravenous). For each mouse, 100 μCi of tracers (100 μL) was injected. The mice were then euthanized at 30 min and 60 min post-injection. The blood in the heart was drawn and an equal column of acetonitrile was added centrifuged for 20 min with 10,000 rpm. The supernatant was collected and another equal column of acetonitrile was added and centrifuged once again. Finally, the supernatant was injected into RP-HPLC for analysis. The area for radioactivity monitoring in the HPLC curve was integrated.

Cell line and animals

The human breast cancer cell line, MDAMB231 (PD-L1 positive) were maintained and passaged in a humidified CO_2 incubator (37°C/5% CO_2) and the cell was cultured in DMEM medium with 10% fetal bovine serum and 0.5% of penicillin/streptomycin.

Male BALB/c *nude-/-* mice and C57BL/6J Jms mice (7-week old) were purchased from Japan SLC (Shizuoka, Japan). All animals received humane care, and the Animal Ethics Committee of the National Institute of Radiological Sciences approved all experiments. All experiments were carried out according to the recommendations of the Committee for the Care and Use of Laboratory Animals, National Institute of Radiological Sciences.

Tumor-bearing models using BALB/c *nude-/-* mice were prepared via a left flank subcutaneous injection of 100 µL of cell (5 × 10^6 cells/mouse). Tumor-bearing mice were used for studies when tumor diameters reached 3-5 mm.

Cellular uptake and inhibition experiment

MDAMB231 cells in 24-well plates (1 × 10^5 cells/well) were maintained for 48 h (37°C/5% CO_2). The medium was removed, and each well was washed three times with phosphate buffered saline (PBS). Radiolabeled tracers in medium (740 KBq/1 mL) was added to each well, and the plates were incubated at 37°C for 5 min, 10 min, 30 min, and 60 min. After incubation, the reaction solution was removed, and each well was washed three times with PBS and the cells were lysed with 0.5 mL NaOH (0.2 mol/L). Radioactivity in cell lysate was measured with the autogamma counter.

Binding inhibition assay was performed using MDAMB231 cells. NOTA-TPP-1 (final concentration: 0, 10, 100, 1000, or 10,000 nmol/L) and radiotracers (74 kBq/1 mL) in medium were added to each well, and the plates were incubated at 37°C for 1 h. After the incubation, cells were treated as they had been for the *in vitro* uptake assay.

Ex vivo biodistribution

A saline solution of tracer (1.85 MBq/200 µL) was injected into C57BL/6J jms mice via the tail vein. Four mice were sacrificed by cervical dislocation at 5 min, 30 min, 60 min, and 120 min after injection for [^{18}F]AlF-PEG-TPP-1. For [^{64}Cu]-TPP-1, the mice were sacrificed at 1 h, 2 h, 4 h, and 20 h. Major organs, including the heart, liver, lung, spleen, pancreas, kidneys, stomach, muscle, small intestine, intestinal lymph node, Testis, muscle, bone, brain, and blood were quickly harvested and weighed. The radioactivity in these organs was measured using the autogamma counter. The results are expressed as the percentage of injected dose per gram of wet tissue (% ID/g). All radioactivity measurements were decay-corrected.

Small-animal PET study

PET scans were conducted using an Inveon PET scanner (Siemens Medical Solutions, Knoxville, TN, USA), which provides 159 transaxial slices with 0.796-mm (center-to-center) spacing, a 10-cm transaxial field of view, and a 12.7-cm axial field of view. Normal C57BL/6J Jms and tumor-bearing BALB/c *nude-/-* mice were kept in the prone position under anesthesia with 1-2% (v/v) isoflurane during the scan. The tracers (14-20 MBq/200-500 μL) were injected via a preinstalled tail vein catheter. Immediately after the injection, a dynamic scan in 3D list mode was acquired for 120 min (C57BL/6J normal mice, n = 3; tumor-bearing mice, n = 3). Maximum intensity projection (MIP) images were obtained for C57BL/6J normal mice and tumor-bearing mice, respectively. PET dynamic images were reconstructed by filtered back projection using Hanning's filter with a Nyquist cutoff of 0.5 cycle/pixel, which was summed using analysis software (ASIPro VM, Siemens Medical Solutions). Volumes of interest, including the heart, kidneys, liver, lung, bone, and tumors, were placed using the ASIPro software. The radioactivity was decay-corrected for the injection time and expressed as the percent of the total injection dose/per gram tissue (%ID/g).

Statistics

All measurements are expressed as means ± standard deviations (SD). Statistical analyses were performed using the GraphPad Prism 5 software (GraphPad Software, La Jolla, CA, USA).

Supplementary Figures and Schemes

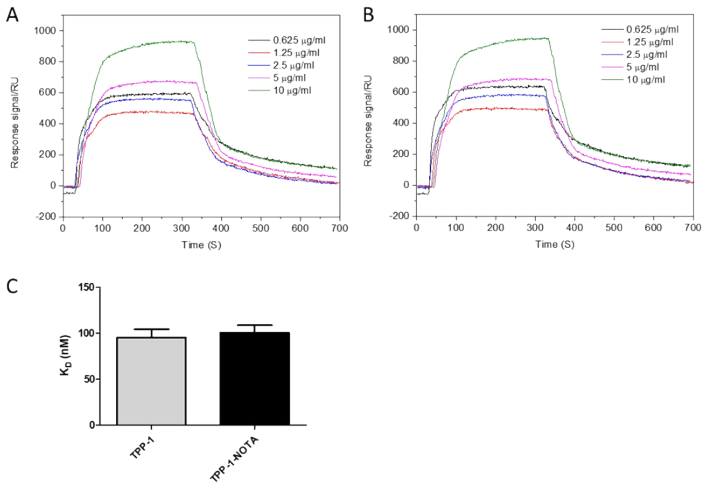

Figure S1. (A-B) The binding affinity of TPP-1 and NOTA-TPP-1 peptide to PD-L1 examined by an SPR method. (C) The calculated K_D values of TPP-1 and NOTA-TPP-1 to PD-L1 protein.

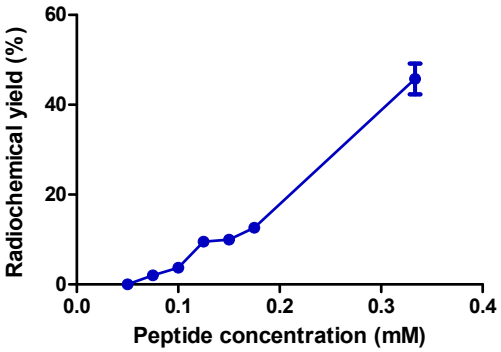

Figure S2. The radiochemical yield of TPP-1 for ^{18}F labeling against different peptide concentrations.

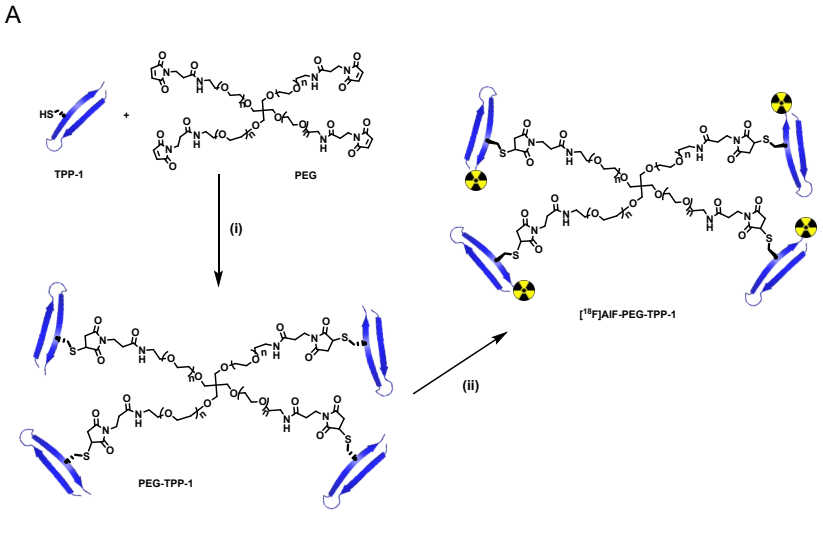

Route	Condition	Solvent	Reaction time (min)	Temperature (℃)	Radiochemical yield %
1	TPP-1-NOTA + [^{18}F]AlF	0.4M NaOAC and ACN (1:1)	10	r.t.	< 5
2		0.4M NaOAC and EtOH (1:1)	10	r.t.	< 5
3		0.4M NaOAC, DMSO	10	100	< 5
4		DMSO	10	100	0.90
5		DMSO	30	100	0.05
6	TPP-1 + PEG + [^{18}F]AlF	Buffer and DMF (2:1)	10	100	0.47
7		Buffer and DMF (2:1)	10 + 20[a]	100, r.t.[b]	0.41

Figure S3. (A) Synthesis of [^{18}F]AlF-PEG-TPP-1 via a two-step strategy. Reaction conditions: (i) PBS: DMSO=1:1 (v/v), r.t., overnight; (ii) corresponding to route 1-5 in Figure S3B. (B) The reaction condition investigated in this study for the synthesis of [^{18}F]AlF-PEG-TPP-1. The routes 6-7 correspond to the 'one-pot' strategy described in Fig. 1B. [a]: The one-pot reaction was divided into two steps, the first step is pre-incubated the [^{18}F]AlF with TPP-1 for 10 min, and then added PEG in the DMF to the reaction mixture for another 20 min reaction. [b]: The reaction temperature corresponds to 100℃ for the chelating reaction and r.t. for the conjugation of TPP-1 with PEG.

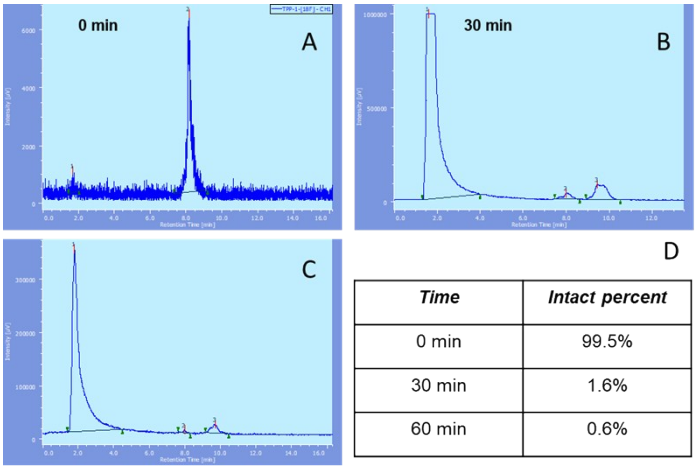

Time	*Intact percent*
0 min	99.5%
30 min	1.6%
60 min	0.6%

Figure S4. (A-C) The RP-HPLC curves for *in vitro* stability measurements of [^{18}F]AlF-TPP-1 at 0 min (A), 30 min (B), and 60 min (C). (D) Summary table of remaining intact tracers in blood after injection for designated times.

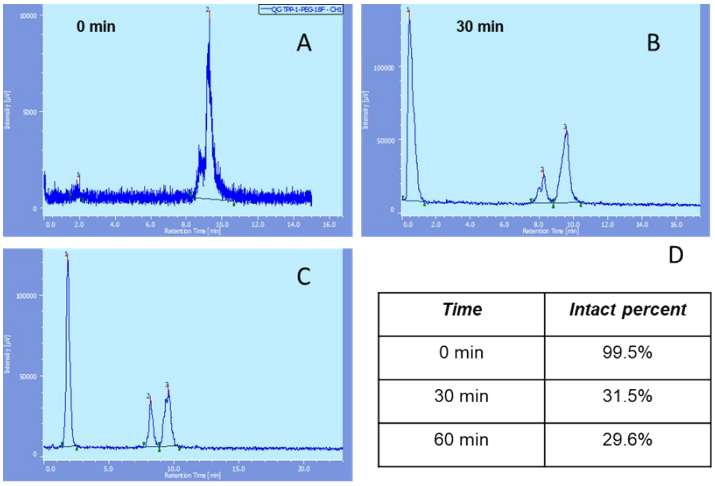

Time	*Intact percent*
0 min	99.5%
30 min	31.5%
60 min	29.6%

Figure S5. (A-C) The RP-HPLC curves for *in vitro* stability measurements of [^{18}F]AlF-PEG-TPP-1 at 0 min (A), 30 min (B), and 60 min (C). (D) Summary table of remaining intact tracers in blood after injection for designated times.

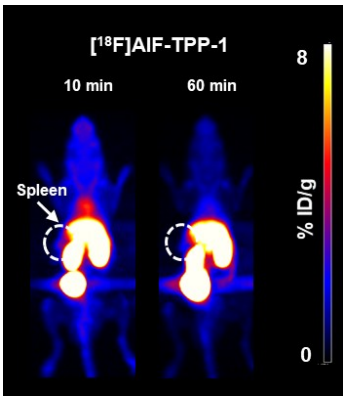

Figure S6. Representative MIPs PET images in C57BL/6 mice at 10 min and 60 min post-injection of tracer [^{18}F]AlF-TPP-1.

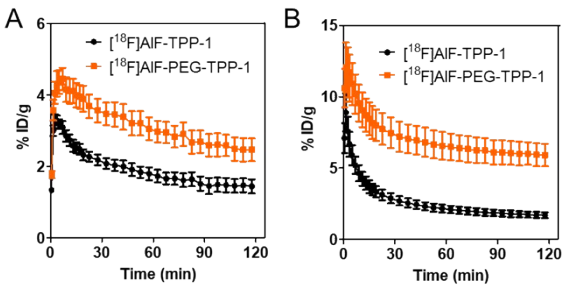

Figure S7. Quantitative uptake of tracers [^{18}F]AlF-TPP-1 and [^{18}F]AlF-PEG-TPP-1 in spleen (B) and heart (C) from PET images. Each data point corresponds to mean ± SD, n≥3.

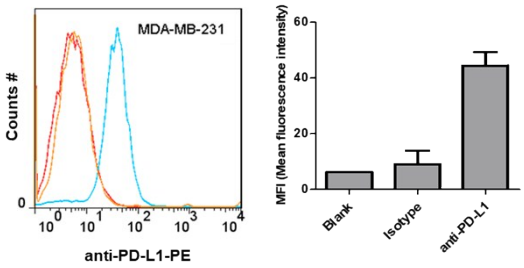

Figure S8. Flow cytometry study of PD-L1 expression in MDA-MB-231 cells.

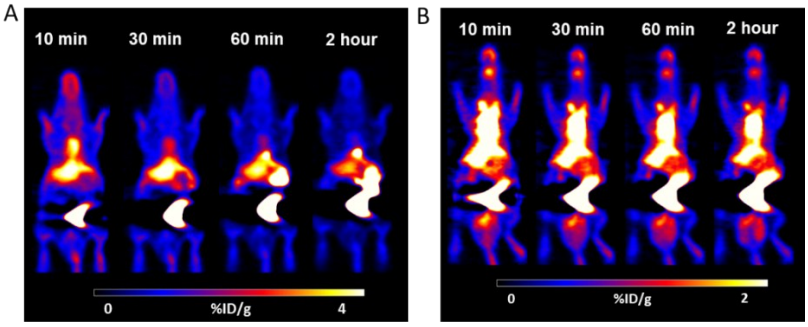

Figure S9. Representative coronal PET images of [^{18}F]AlF-TPP-1 (A) and [^{18}F]AlF-PEG-TPP-1 (B) in MDAMB231 tumor-bearing mice.

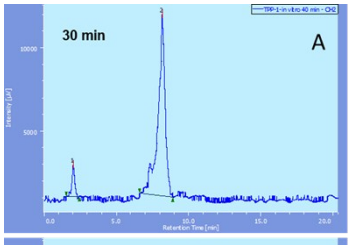

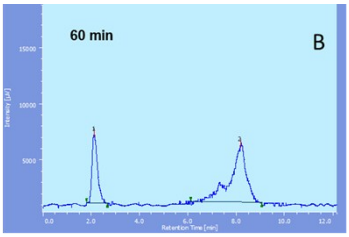

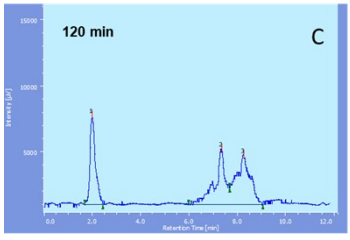

D

Time	*Intact percent*
30 min	93.2%
60 min	71.2%
120 min	39.9%

Figure S10. (A-C) The RP-HPLC curves for *in vitro* stability measurements of [^{64}Cu]-TPP-1 at 30 min (A), 60 min (B), and 120 min (C). (D) Summary table of remaining intact tracers in blood after injection for designated times.

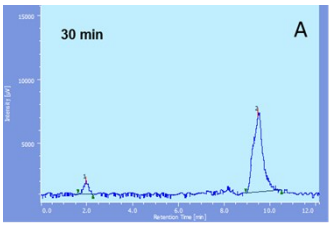

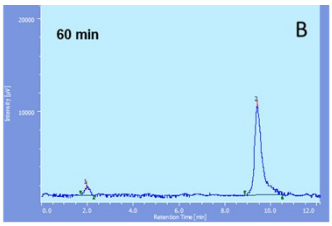

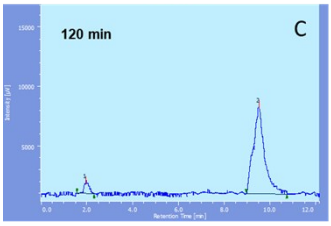

D

Time	*Intact percent*
30 min	92.3%
60 min	92.1%
120 min	92.0%

Figure 11. (A-C) The RP-HPLC curves for *in vitro* stability measurements of [^{64}Cu]-PEG-TPP-1 at 30 min (A), 60 min (B), and 120 min (C). (D) Summary table of remaining intact tracers in blood after injection for designated times.

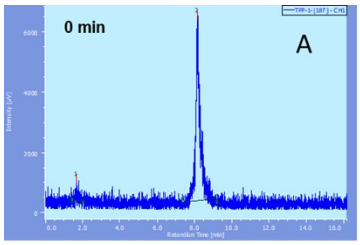

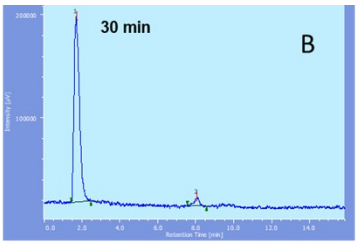

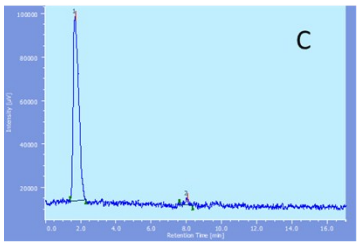

D

Time	*Intact percent*
0 min	99.5%
30 min	4.4%
60 min	2.4%

Figure S12. (A-C) The RP-HPLC curves for *in vivo* stability measurements of [^{18}F]AlF-TPP-1 at 0 min (A), 30 min (B), and 60 min (C). (D) Summary table of remaining intact tracers in blood after injection for designated times.

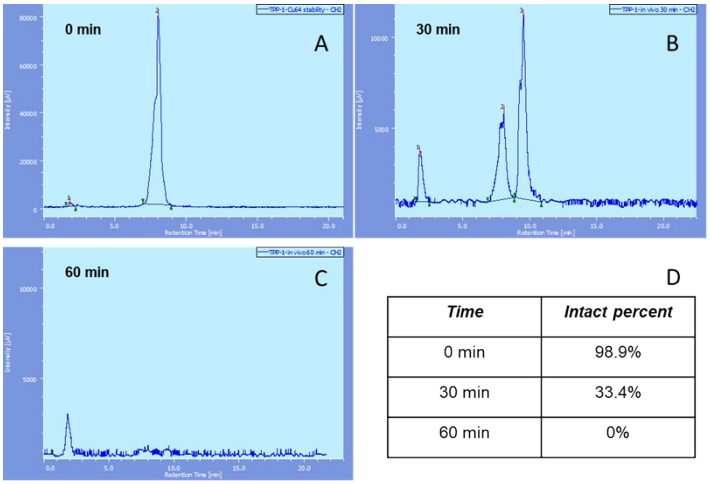

D

Time	*Intact percent*
0 min	98.9%
30 min	33.4%
60 min	0%

Figure S13. (A-C) The RP-HPLC curves for *in vivo* stability measurements of [^{64}Cu]-TPP-1 at 0 min (A), 30 min (B), and 60 min (C). (D) Summary table of remaining intact tracers in blood after injection for designated times.

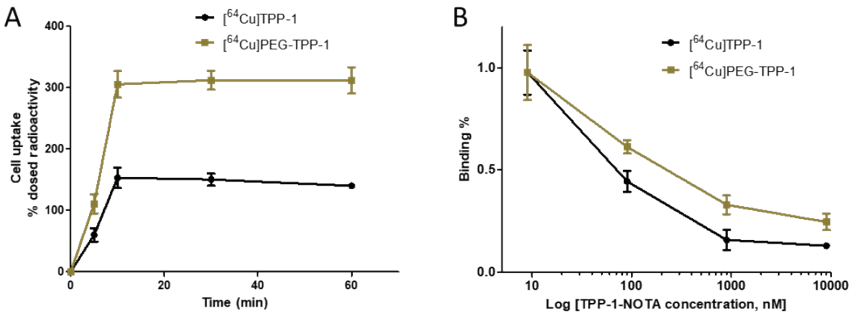

Figure S14. (A) Uptake of [^{64}Cu]-PEG-TPP-1 and [^{64}Cu]-TPP-1 into MDAMB231 cells. (B) Inhibition curve for the uptake of [^{64}Cu]-PEG-TPP-1 and [^{64}Cu]-TPP-1 by MDAMB231 cells at various concentrations of NOTA-TPP-1.

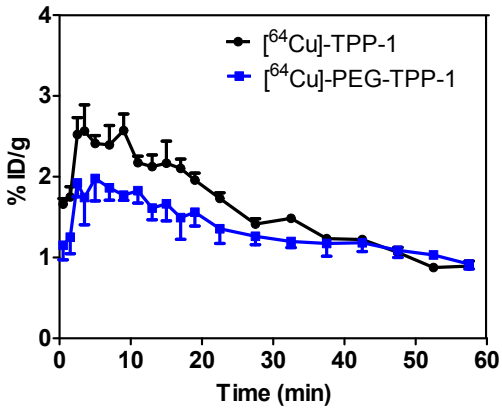

Figure S15. Time activity curves show the tumor uptake in the 60 min post injection of [^{64}Cu]-TPP-1 and [^{64}Cu]-PEG-TPP-1.

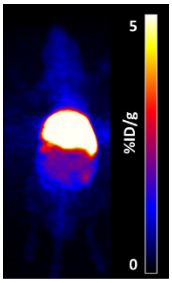

Figure S16. Representative MIPs PET images in C57BL/6 mice at 19 hours post-injection of tracer [^{64}Cu]-anti-PD-L1.

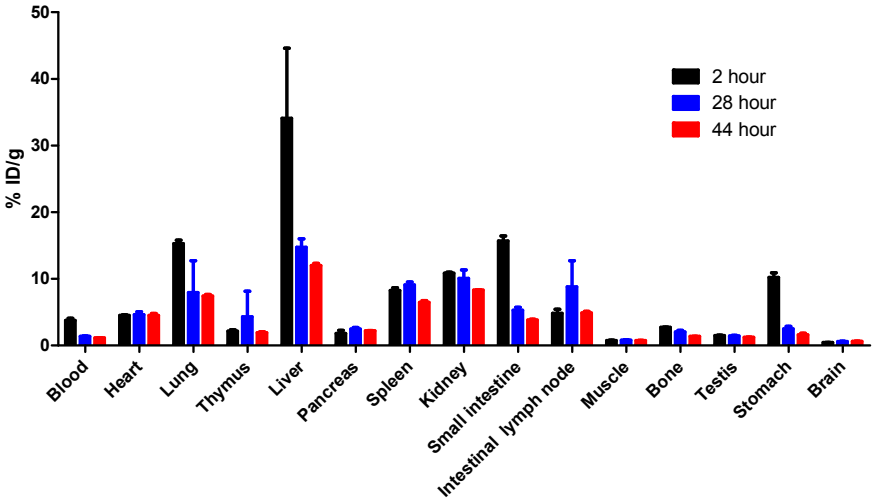

Figure S17. Ex vivo evaluation of [^{64}Cu]-anti-PD-L1 in C57BL/6J mice. The radioactivity in selected organs was measured at 2 hours, 28 hours, and 44 hours post-injection.

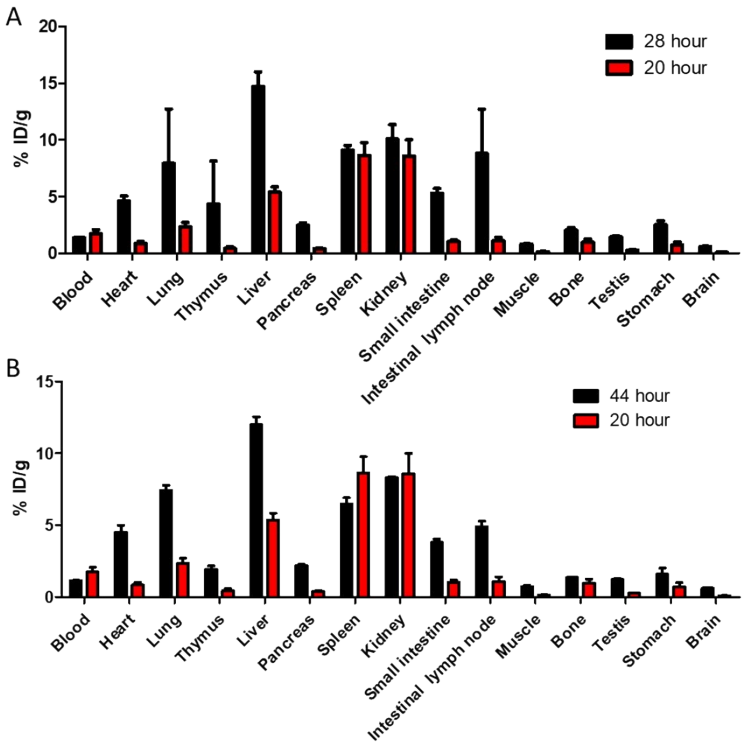

Figure S18. Comparison of radioactivity in major organs at designated time post-injection of [^{64}Cu]-TPP-1 and [^{64}Cu]-anti-PD-L1. (A) A histogram of uptake in major organs of [^{64}Cu]-TPP-1 at 20 hours post-injection and [^{64}Cu]-anti-PD-L1 at 28 hours post-injection. (B) A histogram of uptake in major organs of [^{64}Cu]-TPP-1 at 20 hours post-injection and [^{64}Cu]-anti-PD-L1 at 44 hours post-injection.

Supplementary HPLC chromatogram

The reaction between TPP-1-NOTA and [^{18}F]AlF

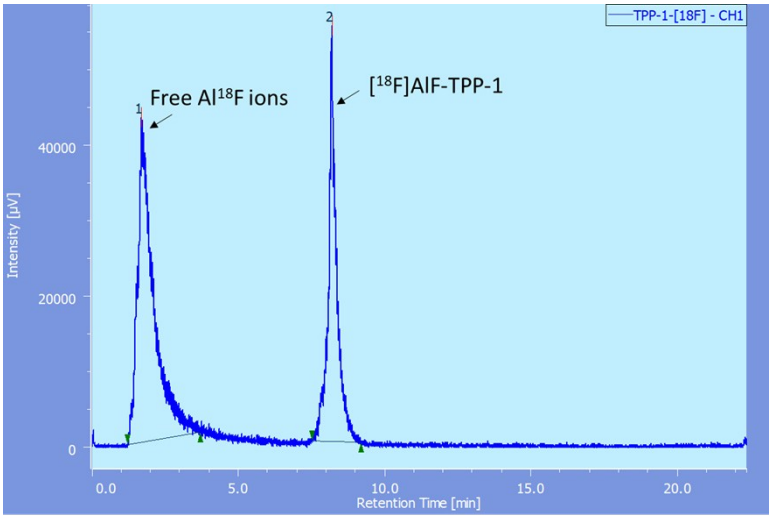

The HPLC chromatogram of purified [^{18}F]AlF-TPP-1

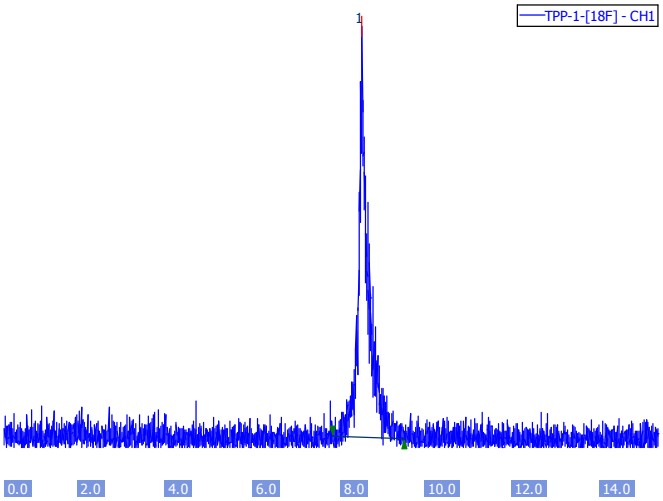

The HPLC chromatogram of purified [^{18}F]AlF-PEG-TPP-1

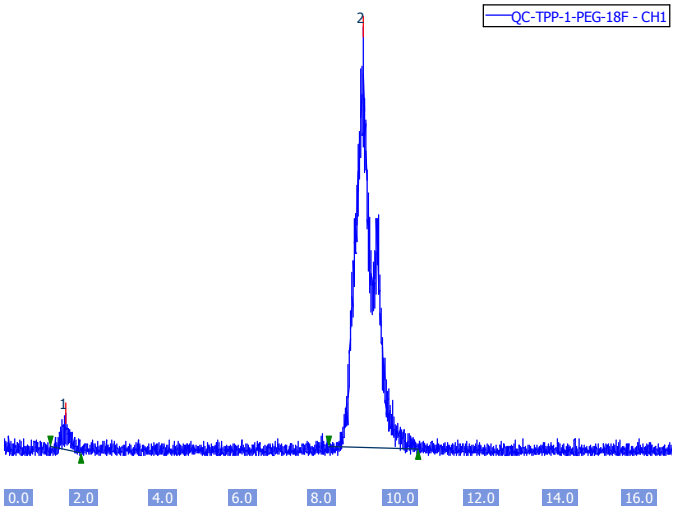

The HPLC chromatogram of purified [^{64}Cu]-TPP-1

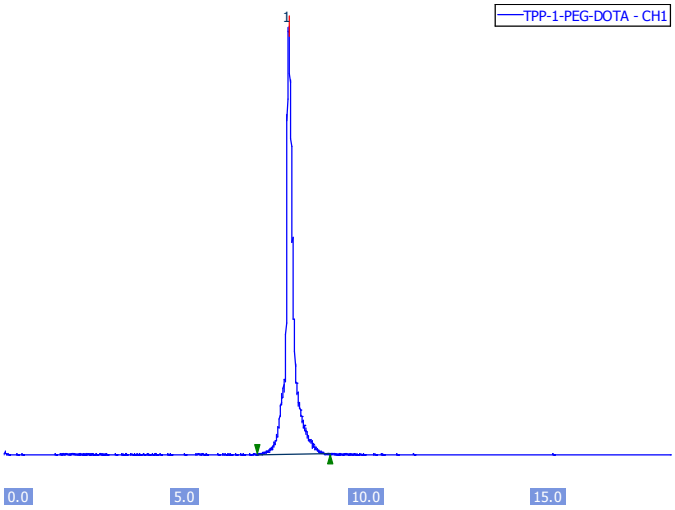

The HPLC chromatogram of purified [^{64}Cu]-PEG-TPP-1

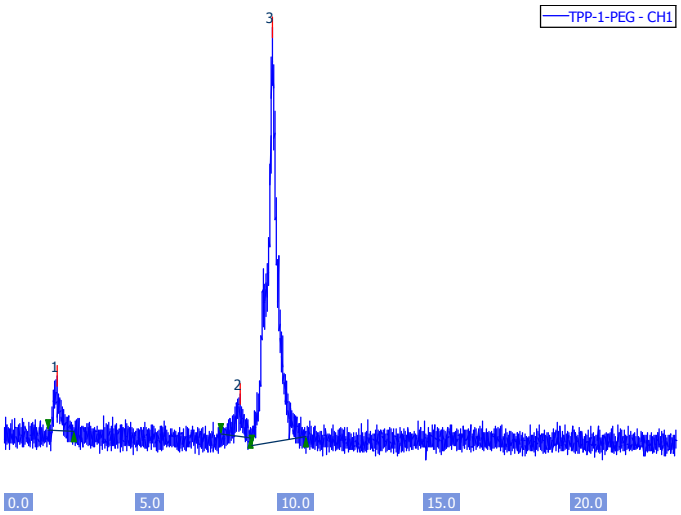

[1] K. Matsumura, M. Zouda, Y. Wada, F. Yamashita, M. Hashida, Y. Watanabe, H. Mukai, *International Journal of Pharmaceutics* **2018**, *545*, 206-214.

[2] N. Bandara, A. Zheleznyak, K. Cherukuri, D. A. Griffith, C. Limberakis, D. A. Tess, C. Jianqing, R. Waterhouse, S. E. Lapi, *Molecular imaging and biology : MIB : the official publication of the Academy of Molecular Imaging* **2016**, *18*, 90-98.